An optoelectronic tweezers system for single cell manipulation and fluorescence imaging of live immune cells

Abigail H. Jeorrett,[1,2]* Steven L. Neale,[3] David Massoubre,[4] Erdan Gu,[2] Robert K. Henderson,[5] Owain Millington,[6] Keith Mathieson,[2] and Martin D. Dawson[2]

[1]*Department of Biomedical Engineering, University of Strathclyde, UK*
[2]*Institute of Photonics, University of Strathclyde, Glasgow, UK*
[3]*School of Engineering, University of Glasgow, Glasgow, UK*
[4]*Queensland Micro and Nanotechnology Centre, Griffith University, Australia*
[5]*Institute for Integrated Micro and Nano Systems, Joint Research Institute for Integrated Systems, The School of Engineering, University of Edinburgh, UK*
[6]*Strathclyde Institute for Pharmacy and Biomedical Sciences, University of Strathclyde, Glasgow, UK*
*abigail.jeorrett@strath.ac.uk

Abstract: A compact optoelectronic tweezers system for combined cell manipulation and analysis is presented. CMOS-controlled gallium nitride micro-LED arrays are used to provide simultaneous spatio-temporal control of dielectrophoresis traps within an optoelectronic tweezers device and fluorescence imaging of contrasting dye labelled cells. This capability provides direct identification, selection and controlled interaction of single T-lymphocytes and dendritic cells. The trap strength and profile for two emission wavelengths of micro-LED array have been measured and a maximum trapping force of 13.1 and 7.6 pN was achieved for projected micro-LED devices emitting at λ_{max} 520 and 450 nm, respectively. A potential application in biological research is demonstrated through the controlled interaction of live immune cells where there is potential for this method of OET to be implemented as a compact device.

OCIS codes: (230.0250) Optoelectronics; (230.3670) Light-emitting diodes; (350.4855) Optical tweezers or optical manipulation; (170.1530) Cell analysis.

References and links

1. J. J. D. McKendry, R. P. Green, A. E. Kelly, Z. Gong, B. Guilhabert, D. Massoubre, E. Gu, and M. D. Dawson, "High-speed visible light communications using individual pixels in a micro light-emitting diode array," IEEE Photon Technol Lett **22**, 1346–1348 (2010).
2. P. Y. Chiou, A. T. Ohta, and M. C. Wu, "Massively parallel manipulation of single cells and microparticles using optical images," Nature **436**, 370–372 (2005).
3. H. Hwang, Y.-J. Choi, W. Choi, S.-H. Kim, J. Jang, and J.-K. Park, "Interactive manipulation of blood cells using a lens-integrated liquid crystal display based optoelectronic tweezers system," Electrophoresis **29**, 1203–1212 (2008).
4. J. K. Valley, M. M. Garcia, P. Swinton, S. L. Neale, H.-Y. Hsu, A. Jamshidi, and M. C. Wu, "Optoelectronic tweezers for quantitative assessment of embryo developmental stage," in *Proceedings of IEEE International Conference on Micro Electro Mechanical Systems (MEMS)* (IEEE, 2010), pp. 943–946.
5. S.-M. Yang, T.-M. Yu, H.-P. Huang, M.-Y. Ku, L. Hsu, and C.-H. Liu, "Dynamic manipulation and patterning of microparticles and cells by using TiOPc-based optoelectronic dielectrophoresis," Opt Lett **35**, 1959–1961 (2010).
6. M. C. Wu, "Optoelectronic tweezers," Nat Photonics **5**, 322–324 (2011).
7. R. Pethig, "Review Article-Dielectrophoresis: Status of the theory, technology, and applications," Biomicrofluidics, **4**, 022811–022835 (2010).
8. A. T. Ohta, P.-Y. Chiou, and M. C. Wu, "Dynamic DMD-driven optoelectronic tweezers for microscopic particle manipulation," in *Conference on Lasers and Electro-Optics/International Quantum Electronics Conference and Photonic Applications Systems Technologies*, Vol. 1 of 2004 OSA Technical Digest Series (Optical Society of America, 2004), paper CWS5.

9.   A. Zarowna-Dabrowska, S. L. Neale, D. Massoubre, J. J. D. McKendry, B. R. Rae, R. K. Henderson, M. J. Rose, H. Yin, J. M. Cooper, E. Gu, and M. D. Dawson, "Miniaturized optoelectronic tweezers controlled by GaN micro-pixel light emitting diode arrays," Opt Express, **19**, 2720–2728 (2011).

10. H. Y. Hsu, A. T. Ohta, P. Y. Chiou, A. Jamshidi, and M. C. Wu, "Phototransistor-based Optoelectronic Tweezers for Cell Manipulation in Highly Conductive Solution," in Proceedings of Solid-State Sensors, Actuators and Microsystems International Conference, Transducers, 2007, pp. 477–480.

11. A. Grakoui, S. K. Bromley, C. Sumen, M. M. Davis, A. S. Shaw, P. M. Allen, and M. L. Dustin, "The Immunological Synapse: A Molecular Machine Controlling T-Cell Activation," Science, **285**, 221–227 (1999).

12. J. K. Valley, A. Jamshidi, A. T. Ohta, H.-Y. Hsu, and M. C. Wu, "Operational regimes and physics present in optoelectronic tweezers," J Microelectromech Syst, **17**, 342–350 (2008).

13. B.R. Rae, C. Griffin, J. J. D. McKendry, J. M. Girkin, H. X. Zhang, E. Gu, D. Renshaw, E. Charbon, M. D. Dawson, and R. K. Henderson, "CMOS driven micro-pixel LEDs integrated with single photon avalanche diodes for time resolved fluorescence measurements," J Phys D: Appl Phys, **41**, 094011 (2008).

14. D. M. Underhill, M. Bassetti, A. Rudensky, and A. Aderem, "Dynamic interactions of macrophages with T cells during antigen presentation," J Exp Med, **190**, 1909–1914 (1999).

15. M. B. Lutz, N. Kukutsch, A. L. J. Ogilvie, S. Rössner, F. Koch, N. Romani, and G. Schuler, "An advanced culture method for generating large quantities of highly pure dendritic cells from mouse bone marrow," J Immunol Methods, **223**, 77–92 (1999).

16. Life Technology, "CellTracker™ Probes for Long-Term Tracing of Living Cells," http://tools.invitrogen.com/content/sfs/manuals/mp02925.pdf

17. M. P. Hughes, *Nanoelectromechanics in Engineering and Biology* (CRC Press, 2003).

18. K. Svoboda and S. M. Block, "Biological applications of optical forces," Annu Rev Biophys Biomol Struct, **23**, 247–285 (1994).

19. S. L. Neale, A. T. Ohta, H.-Y. Hsu, J. K. Valley, A. Jamshidi and M. C. Wu, "Trap profiles of projector based optoelectronic tweezers (OET) with HeLa cells," Opt Express, **17**, 5232–39 (2009).

20. T. Kamei, B. M. Paegel, J. R. Scherer, A. M. Skelley, R. A. Street, and R. A. Mathies, "Integrated Hydrogenated amorphous Si photodiode detector for microfluidic bioanalytical devices," Anal Chem, **75**, 5300–5305 (2003).

21. S. L. Neale, M. Mazilu, J. I. B. Wilson, K. Dholakia, and T. F. Krauss, "The resolution of optical traps created by Light Induced Dielectrophoresis (LIDEP)," Opt Express, **15**, 12619–12626 (2007).

22. K. K. Ghosh, L. D. Burns, E. D. Cocker, A. Nimmeriahn, Y. Ziv, A. El Gamal, Schnitzer, 'Miniaturized integration of a fluorescence microscope' Nat Methods **8**, 871–8 (2011

1. Introduction

Manipulation of cellular-scale particles is an essential technique in cell biology for separation, sorting and control of intercellular interactions. In this study, an optoelectronic tweezers (OET) system for single cell manipulation and fluorescence imaging was developed and its capabilities and operation are reported. Our system is based on CMOS-controlled gallium nitride (GaN) micro-light-emitting diode (micro-LED) arrays [1] projected onto an OET device, where we take advantage of novel high fill-factor 'chequerboard' format micro-LED arrays as shown in Fig. 1(a) to achieve a high level of manipulation and functionality. To our knowledge, this is the first demonstration of combining manipulation *and* fluorescence imaging using the same compact light source, paving the way for a compact integrated instrument for cell manipulation and analysis.

Optoelectronic tweezers (OET) have developed over the last decade as an alternative to established cell manipulation techniques. OET combines optical patterning and electric field gradients to trap cells [2–6]. An OET device shown in Fig. 1(b) typically consists of an upper and a lower glass slide coated with a transparent conductor (typically indium tin oxide, ITO) with the lower slide coated with an additional photoconductive layer. A light pattern is projected onto the device which creates 'virtual electrodes' used to corral particles via dielectrophoresis (DEP) [7]. OET is a method of light-induced dielectrophoresis where low intensity (μW), incoherent light can be used.
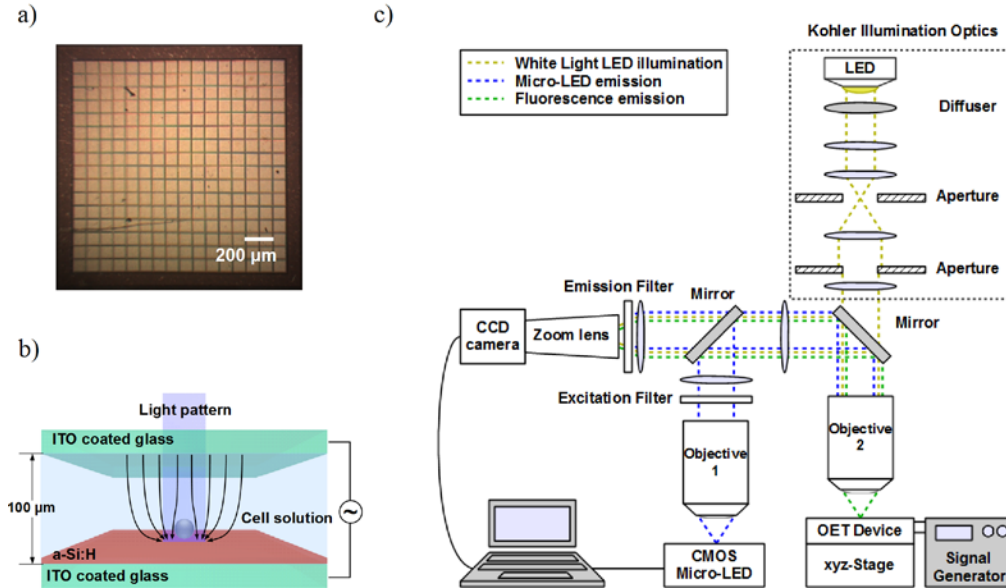
Fig. 1. a) Photograph of chequerboard array of 16 x 16 micro-LED pixels 99 x 99μm, on a pitch of 100 μm; b) schematic of an OET device consisting of two opposing ITO coated glass slides with an additional layer of a photoconductor (amorphous silicon, a-Si:H) deposited onto the lower slide. 'Virtual electrodes' are created within the device when a light pattern is focused onto the photoconductive surface; and c) schematic of the micro-LED projection system consisting of two microscope objectives to reduce the size of pixels imaged onto the OET device.

OET systems typically use a liquid crystal display (LCD) and a spatial light modulator (SLM) [3] or a digital light projector (DLP) [8] to create the light pattern. More recently, a CMOS-controlled GaN micro-LED array has been used to achieve cluster patterns of cells via OET [9]. In our study, a projection system was built using CMOS-controlled micro-LED arrays to achieve single cell manipulation *and* excitation of fluorescence from fluorescently-labelled cells. CMOS technology provides compact control and individual-addressability for dynamic patterning of micro-LED arrays. These arrays provide a compact low power illumination source, in a range of emission wavelengths, to give scalability and reduce thermal damage to biological samples. The micro-LED array is projected onto the OET device via two objective lens as shown in Fig. 1(c), reducing the pixel size used to activate each trap. While manipulation of cells via OET and excitation of fluorescence has been shown before [10] this is, to our knowledge, the first demonstration of single cell manipulation *and* fluorescence imaging using the same illumination source where two emission wavelengths have been investigated.

As proof of concept, immune cells were used to demonstrate the potential application of this technology in medical research. The interaction of T-lymphocytes and dendritic cells is widely studied in order to investigate the factors affecting the activation of T-lymphocytes during and following infection or vaccination. The role of dendritic cells is to present antigen to T-lymphocytes which results in the formation of an immunological synapse, the strength and duration of which gives rise to a particular immune response [11]. Observing and controlling these interactions requires a tool that provides 'gentle' manipulation of these cells to precisely control the contact between individual pairs of dendritic cells and T-lymphocytes. Such a device must be able to monitor these interactions and track activation over time, often using fluorescence-based reporter systems. A compact, simple tool combining these functionalities would provide an approach for controlling and measuring the force of cell interactions providing additional information to pharmaceutical research scientists, potentially speeding up and reducing the cost of the drug discovery process.

Initial measurement of the DEP force on T-lymphocytes (DO11.10 cell line) was carried out where a maximum force of 13.1 pN was found using a micro-LED array with an emission wavelength of 520 nm. Identification of different cell types was confirmed via fluorescence imaging. Importantly, this approach allows for selection and controlled interaction of T-lymphocytes and dendritic cells which has not been achieved previously using OET. These results demonstrate the feasibility of 'chequerboard' micro-LED arrays for single cell manipulation and fluorescence analysis and pave the way for the development of a novel, integrated and compact instrument.

2. Materials and methods

2.1 OET and DEP

A projection system [Fig. 1(c)] was used here to activate potential energy traps within the OET device for cell manipulation. The OET device [Fig. 1(b)] comprises an upper glass slide coated with ITO and a lower electrode coated with ITO and a 300 nm thick layer of hydrogenated amorphous silicon (a-Si:H) deposited using plasma enhanced chemical vapour deposition. Electrical contact was made to each ITO layer through a wire connected by conductive epoxy. A function generator (Aim-TTi TG315) was used to apply an AC voltage across the OET device. A light pattern is used to illuminate the a-Si:H surface of the lower slide which generates a non-uniform electric field within which cells can be manipulated by DEP. If the effective permittivity of the particles is greater than the liquid layer, an attractive DEP force is achieved. If the permittivity of the particles is less than the liquid layer, the reverse is true, as defined by the real part of the Clausius-Mossotti factor Re[CM] (Eq. (2) in [12]), which governs the direction of the force in the standard equation for dielectrophoresis [7]:

$$F_{DEP} = 2\pi\varepsilon_m R^3 \, \text{Re}[CM](\nabla E^2) \qquad (1)$$

Here ε_m is the permittivity of the medium, R is the radius of the particle, and ∇E^2 is the gradient of the electric field squared. The maximum electric field gradient, and so the maximum DEP force on suspended cells, acts at the edge of the illuminated region, also shown in [9].

2.2 CMOS-driven micro-LED arrays

The micro-LED arrays used here are custom fabricated and are described elsewhere [1]. In [9], circular pixels of varying diameter were turned on and the movement of cells, in response to the generated OET forces, was monitored over long distances. The micro-LED arrays used here feature several advantages over those used before. The new generation of arrays provides an increased fill-factor due to the use of square pixels of size 99 x 99 µm^2 on a pitch of 100 µm, resulting in a gap of only 1 µm between adjacent pixels as shown in Fig. 1(a). The pixels are individually addressable and programmable since each one of the 16 x 16 micro-LED pixels has its own CMOS driver, which allows individual cells to be trapped and moved to a specific location and isolated from nearby cells. The CMOS-chip [13] is powered and controlled through a FPGA integration module (Opal Kelly, Portland, USA) which connects via USB to a PC. Two micro-LED devices of different emission wavelength (λ_{max} 450 nm and 520 nm) were employed, both of which are 16 x 16 array of square 'chequerboard' pixels.

2.3 OET set-up

The pitch between two adjacent CMOS-bonded micro-LED pixels is limited by the minimum pitch of the CMOS-driver circuits, which in turn is limited by the bump bonding process. The projection system [Fig. 1(c)] reduces the size of the micro-LED array by a factor of 2 or 4 depending on the ratio of the magnifications of Objective 1 and 2 where the magnification of Objective 1 is less than Objective 2. In order to view the cells in sufficient detail, while

achieving a 4 times de-magnification of the micro-LED array, it was necessary to use a 10x objective to image the micro-LED device (Objective 1, NA 0.25) and 40x objective to image cells (Objective 2, NA 0.75). The low NA of the collection objective and the high divergence angle of the micro-LEDs reduced the optical power at the sample. In order to achieve a 2 times de-magnification of the micro-LED array the 10x objective was used with a 20x objective at Objective 2.

The CMOS-micro-LED device is placed in front of Objective 1 and the OET device is placed in front of Objective 2 on an xyz-translation stage [Fig. 1(c)]. The micro-LED array is coupled into the OET device via two mirrors and a 4f optical system was used to maintain the integrity of the projected micro-LED pattern. Köhler illumination optics were used to provide even illumination to the sample from a standard white light LED.

A CCD camera (QICAM Fast 1394, QI Imaging) and a zoom lens (Navatar ZOOM 7000E) were used to image the sample [Fig. 1(c)]. An excitation filter (500 nm long-pass) was used to remove the green tail of the micro-LED device emitting at λ_{max} 450 nm during fluorescence imaging. An emission filter (520 nm long-pass) was used to reduce the intensity of the micro-LED emission, relative to bright field illumination provided by the white light LED, and to allow transmission of fluorescence from dye-labelled cells.

The output power of the device emitting at λ_{max} 450 nm was 2.5 mW (at 54 mA) providing 0.48 or 0.17 W/cm^2 power at the sample for 25 or 50 μm imaged pixel size, respectively. The device emitting at λ_{max} 520 nm had an output power of 0.9 mW (at 44 mA) providing 0.09 W/cm^2 power at the sample for 25 μm imaged pixel size. A voltage of 4.9 V was applied to both devices.

2.4 Cell preparation

The DO11.10 T-lymphocyte hybridoma cell line, modified to express EGFP (enhanced green fluorescent protein) following NFAT-activation [14], was cultured in RPMI 1640 medium supplemented with fetal calf serum (10 %), penicillin and streptomycin. Primary dendritic cells were obtained by culturing cells extracted from the bone marrow of BALB/c mice with granulocyte-macrophage colony-stimulating factor (GM-CSF) for 1 week prior to use [15]. Carboxyfluorescien diacetate succinimidyl ester (CFSE) or Cell Tracker Orange (both Life Technologies Corporation) labeling was carried out at a final concentration of 10 or 25 μM, respectively [16]. All cell suspensions were washed 3 times in isotonic sugar solution (8.5 % sucrose and 0.3 % dextrose) and re-suspended to a final concentration of $2x10^5$ cells/ml or $1.5x10^5$ cells/ml for single or mixed populations, respectively.

2.5 Measurement of cell velocity and trap profile

The velocity and trap profile of T-cells was measured using a viscous drag method where Stokes' Law was used to calculate the DEP force [17]:

$$\vec{v} = \frac{F_{DEP}}{6\pi\eta r} \qquad (2)$$

Here η is the viscosity of the liquid and ν is a velocity of the particle with radius r when the velocity vector is parallel to the gradient of the electric-field. A motorised stage (CONEX-LTA-HS, Newport) was used to increase the velocity of the OET device, relative to the fixed micro-LED array, until a single T-cell remained trapped at a maximum distance from the centre of a single projected pixel. The viscous drag force is balanced by the DEP force when this state is achieved and the DEP force can then be calculated using Stokes Law. The force profile of a single pixel trap was determined by measuring the position of a cell, relative to the centre of the trap, at varying applied forces (stage velocities) to obtain a plot of the force experienced by a cell at varying locations in a single pixel trap. Faxen's correction [18] was used here as the trapped cell was close to the lower electrode of the OET device as evidenced by imaging of trapped cells in a different plane of focus relative to un-trapped cells. The height above the a-Si:H is assumed to be equal to the average radius of the cells.

3. Results

3.1 OET trap characterisation for T-lymphocytes

The DEP force increases with the square of the applied electric field [Fig. 2(a)], as predicted by the DEP equation [Eq. (1)] where the electric field gradient squared is directly proportional to the applied electric field squared. The error bars are due to variations in cell size and morphology. A maximum average DEP force exerted on T-lymphocytes of 13.1 pN (45 μm/s) was achieved using the micro-LED device with λ_{max} at 520 nm, at a projected pixel size of 25 μm. A maximum average DEP force on T-lymphocytes of 7.6 pN (26 μm/s) and 5.1 pN (17.4 μm/s) was achieved using the micro-LED emitting at λ_{max} 450 nm at a projected pixel size of 25 and 50 μm, respectively. A cross-section of the trapping force experienced by T-lymphocytes was compared for each of the micro-LED arrays and the trap stiffness calculated using the gradient of a linear fit to each curve [Fig. 2(b)]. A trap stiffness of 6.7×10^{-7} N/m was achieved using the micro-LED with λ_{max} at 520 nm, at a projected pixel size of 25 μm. A trap stiffness of 2.5×10^{-7} and 0.2×10^{-7} was achieved using the micro-LED device emitting at λ_{max} 450 nm, at a projected pixel size of 25 and 50 μm, respectively.
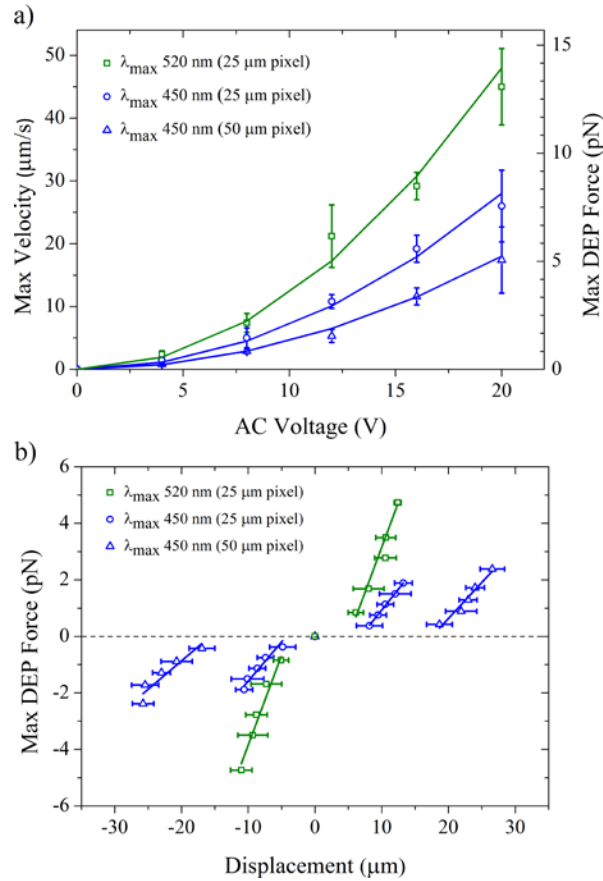

Fig. 2. a) Plot of the max average T-lymphocyte velocity (n=5 per data points) as a function of applied voltage at 30 kHz with corresponding quadratic fits; b) plot of max average T-lymphocyte displacement (n=5 per data points) at varying applied forces at 20 V_{p-p} applied voltage (30 kHz) with corresponding linear fits. Error bars represent +/- 1σ.

The measured values of velocity (DEP force) are comparable to those reported elsewhere for the manipulation of cells, via OET systems which incorporate DLP to project a light pattern onto the OET device [19]. Trap stiffness was 4 times lower, however larger traps were used in this study.

3.2 OET manipulation and fluorescence imaging of cells

Manipulation and fluorescence imaging was achieved for individual populations of T-lymphocytes and dendritic cells using animated light patterns as shown in Fig. 3.
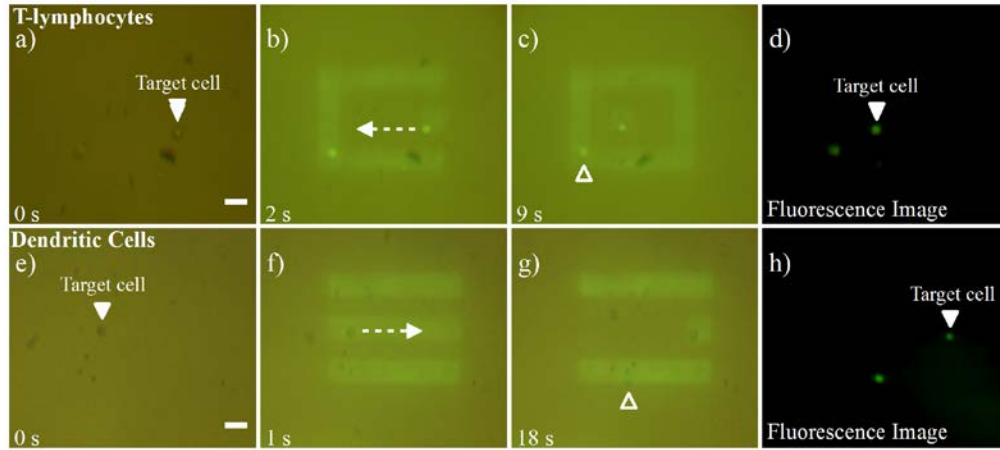

Fig. 3. Selected frames from Media 1 and Media 2 showing trapping of live immune cells using a λ_{max} 450 nm micro-LED array at 25 μm projected pixel size was used. Frames captured during trapping of a targeted T-lymphocyte and dendritic cell are shown in a)-d) and e)-h), respectively; a) and e) before micro-LED pattern turn on; b) and f) immediately after the start of a pixel animation; c) and g) after pixel animation; d) and h) fluorescence image showing CFSE labelled cells after pixel animation. Applied voltage 20 V_{p-p}, 30 kHz. Scale bar (shown in a) and e)) is 25 μm.

Both T-lymphocytes and dendritic cells experience positive DEP in the OET device and targeted cells (solid arrowhead, Figs. 3(a) and 3(e)) follow the path of a single illuminated pixel (dashed arrow, Figs. 3(b) and 3(f)) into a light cage while other cells (hollow arrowhead, Figs. 3(c) and 3(g)) are prevented from interfering with the target cell by the walls of the light cage. Subsequently, identification of the cells was achieved via fluorescence imaging. These examples show the potential for sophisticated single cell control and array formation of immune cells with the potential to reveal subsequent cell function using fluorescence-based assays.

3.3 Identification and controlled interaction of cells in a mixed population

The λ_{max} 450 nm micro-LED device was shown to excite fluorescence of contrasting fluorescent dyes, which could be used to distinguish T-lymphocytes (labelled with Cell Tracker Orange) and dendritic cells (labelled with CFSE) in a mixed population [Fig. 4]. Critically, using a 1:1 mixture of T-lymphocytes and dendritic cells, the micro-LED device was able to specifically control the interactions between two cells, initially manipulating them to bring them into contact [Figs. 4(d)-4(e)] and then subsequently terminating cell-cell interaction [Fig. 4(f)].
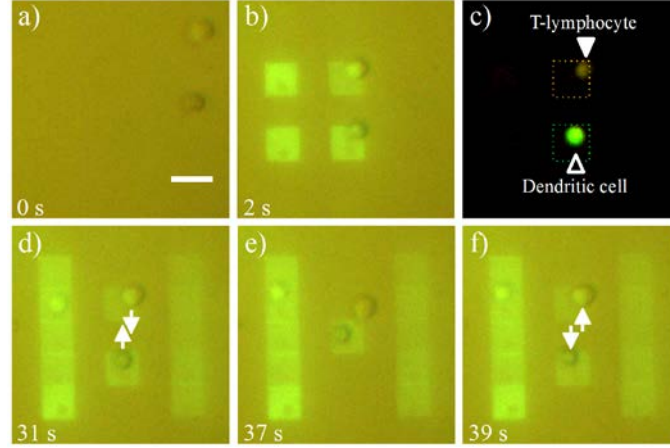
Fig. 4. Image sequence showing trapping, identification and controlled single cell interaction of T-lymphocytes and dendritic cells with a λ_{max} 450 nm micro-LED array at a projected pixel size of 25 μm; a) before micro-LED turn on (0 s); b) after micro-LED turn on (2 s); c) fluorescence image showing T-lymphocyte (orange, solid arrowhead) and dendritic cell (green, hollow arrowhead); d) first frame of pixel animation as cells are manipulated into contact (31 s); e) second frame of pixel animation as cells interact (37 s); f) final frame of pixel animation in which cell-contact is interrupted (39 s). Applied voltage 20 V_{p-p}, 30 kHz. Scale bar is 25 μm.

4. Discussion

In this paper, a novel and compact OET system has been built which provides single cell manipulation with simultaneous fluorescence imaging. The velocity of T-lymphocytes and dendritic cells within the system was characterized using micro-LED devices with λ_{max} at 450 and 520 nm, respectively.

The force experienced by both cell types was a positive DEP force for the conditions applied (20 V, 30 kHz). The OET force is dictated by the electronic properties and morphology of the cell and as these cell types are similar in both respects, it is not surprising that a similar force should be exerted on both. The force on T-lymphocytes was shown to be in agreement with the DEP force equation where the force increased with the square of the applied voltage at constant applied AC frequency. This is shown by the quadratic fit of the voltage profile curves and suggests the force experienced by cells is predominately a close range DEP force and contributions from alternative forces (e.g. light-actuated AC electro-osmosis, electro-thermal effects) are minimal, as is the case in typical OET manipulation schemes [12]. DEP is advantageous for this application as it provides tight control of cells and there is little interference from cells hundreds of microns from the illuminated pixels. Those cells which are in close proximity to the pixel pattern can be easily captured and retained at a sufficient distance from isolated cells of interest. The force of cell interaction could be measured by first calibrating the OET trap by varying m-LED powers and measuring the force experienced by single cells. The intensity of light required to separate interacting cells could then be used to determine the force of interaction.

The output power of the micro-LED array emitting at λ_{max} 520 nm was lower than that of the λ_{max} 450 nm emitting device (by 2 times) however a maximum DEP force (13.1 pN) and trap stiffness (6.7×10^{-7} N/m) was achieved using the longer wavelength device which is comparable to reported OET set-ups which utilize a DLP to achieve traps. The absorption coefficient of a-Si:H at 450 nm is 5×10^5 cm^{-1} [20] which is 5 times that at 520 nm so in this case, longer wavelengths of light propagate further through the a-Si:H to the conductive ITO layer, increasing the electric field strength at the edge of the illuminated region, therefore producing a greater trapping force and trap stiffness. In applications where a higher trapping force is required (e.g. formation of strong immunological synapse) the trapping force may be increased with improved fabrication techniques of the micro-LED devices. The size of the

OET traps created were the same size as the projected pixel used to actuate the trap which is typically the case for positive OET where the cells are attracted to a region of high electric field gradient located within the illuminated region of a-Si:H. If smaller traps are required it would be necessary to reduce the size of the projected pixels at the device which could be achieved through the development of finer pitched micro-LED arrays or by changing the focusing optics of the optical setup to increase the de-magnification of the arrays onto the OET device [21].

Single cell manipulation and fluorescence excitation was demonstrated for T-lymphocyte and dendritic cell populations using the device emitting at λ_{max} 450 nm where it was possible to excite a range of fluorescent dyes. Programmed pixel animations were used to select and isolate a single cell and fluorescence from labelled cells (CFSE and Cell Tracker Orange) allowed for identification of different cell types after OET manipulation. This demonstrates the ability of the system to perform manipulation on a single cell level with a similar level of control to that of other OET systems [3] but with the added benefit of fluorescence excitation in a compact format, eliminating the need for separate OET and fluorescence illumination sources, which is typically the case.

The combination of fluorescence identification and OET driven manipulation was then used to separate and identify cell type in a mixed population of immune cells. Whilst fluorescence yield of Cell Tracker Orange-labelled cells was low in our set-up relative to that of CFSE, increased micro-LED output power may aid identification of labelled cells using the device emitting at λ_{max} 450 nm array. The interaction of a single pair of cells, one from each population, was demonstrated using an animated light pattern. The set-up has demonstrated the potential of CMOS-micro-LED devices for use in large scale, programmable array formation, which could be used in the identification and controlled single cell manipulation of a range of cell types.

5. Conclusion

A compact, integrated OET system has been characterized and demonstrated for micro-manipulation and fluorescence identification of cells, applied in this case to the interaction of T-lymphocytes and dendritic cells. CMOS-controlled GaN micro-LED arrays were successfully used to create the OET system where a projected pattern of micro-LEDs was used to generate a dynamic potential landscape for trapping via DEP (maximum trapping force of 13.1 pN using a micro-LED device emitting at λ_{max} 520 nm) and excite fluorescence from dye labelled cells using a micro-LED device emitting at λ_{max} 450 nm. Individual addressability and pattern programmability of the arrays allowed reconfiguration based on a desired application as demonstrated in the isolation of a single cell from a single population and the collection and controlled interaction of single cells in a mixed population. This system provides a compact, micro-manipulation tool which can be applied to investigate T-lymphocyte activation and other applications involving single cell manipulation and fluorescence imaging of cells. In order for this system to be developed into a compact tool to provide a convenient hand-held device for the investigation of cell-cell interactions there are several steps to take. Current work is focused on integrating a micro-LED device and an OET device into a single chip which can be easily transported and viewed under a standard microscope. Recent advances in the miniaturization of microscope optics by Gosh et al. [22] show that there is potential to create a fully integrated, self-contained and portable system. Fluorescence imaging is currently an issue due to high absorption of light by a-Si:H however, reducing the thickness or patterning the amorphous silicon could provide fluorescence imaging *and* cell manipulation driven by m-LED arrays in a single compact device.

Acknowledgments